

# Analysis of Near-field Tip Vortex behind an Untwisted Rectangular Wing

Sanjay Kumar Sardiwal, Narote Mounika, C.Agnihotra Reddy, ND. Nicholas

**Abstract**— Numerical simulations of the flow around an unswept and untwisted rectangular wing (NACA 0012) with rounded tip are carried out at a high geometric angle of attack 10 degrees using the finite-volume based the commercial Computational Fluid Dynamics (CFD) code FLUENT. Wingtip vortices influence the induced drag for a three-dimensional wing. So, it is important to study the characteristics of wing tip vortices in order to reduce the induced drag. The numerical results of pressure coefficient and axial velocity were obtained by using the CFD code show a good agreement with the experimental data. The variation of circulation at different areas to the right of the wingtip vortex core and the strength of the circulation around the vortex core are computed. Also the tangential velocities at one chord downstream of the trailing edge are evaluated

**Index Terms**— Tip-vortex; Drag; Circulation; Tangential velocity.

## I. INTRODUCTION

Wing tip-vortex flow around lifting surfaces such as wings and propeller blades has long been a topic of both fundamental and practical interest in the aerospace industry for its impact on various aspects of aerodynamic performance. The investigation of trailing vortices is an important task in aerodynamics because of their influence on following aircraft and because of the energy contained in these vortices, which is directly related to induced drag. Achieving this desired accuracy is a demanding task, since high grid resolution is necessary at the wing's boundary and in the vortex region, where velocity gradients are high. Consequently, this leads to high numbers of cells and to very long stretched cells at the wall boundaries.

In a finite wing, there is an opportunity for the pressures acting on the upper and lower surfaces to interact near the wing tip [1](Fig. 1). The shorter the distance between the wing tip, the larger the downwash velocity and the induced drag [2]. The trailing vortex system also generates an upwash in the regions beyond the wing span and a downwash inside the wing span. This downwash produced by the trailing vortex system adds to the downwash produced by the bound vortex system [3] (Fig. 2).

**Manuscript received September 03, 2014.**

**Sanjay Kumar Sardiwal**, Department of Aeronautical Engineering, MLR Institute of Technology, Hyderabad

**Narote Mounika**, Department of Aeronautical Engineering, MLR Institute of Technology, Hyderabad

**C.Agnihotra Reddy**, Department of Aeronautical Engineering, MLR Institute of Technology, Hyderabad

**ND. Nicholas**, Department of Aeronautical Engineering, MLR Institute of Technology, Hyderabad.

Aerodynamic efficiency can be improved by increasing the maximum lift-to-drag ratio at the cruise flight condition. Because induced drag is typically 30 percent or more of the total drag on a subsonic transport in cruising flight [4]. A 10% drag reduction on a large military transport aircraft is estimated to save up to 13 million gallons of fuel over its lifetime [5]. The world total jet fleet is estimated to be around 17 thousand aircraft [6]. Such reduction in drag could result in fuel savings in fuel up to 1x10<sup>10</sup> U.S. dollars (\$). This drag is even more significant at low speed, during take-off conditions, where it can account for 80-90% of the aircraft drag [7].

Besides the advantage of lowering operating costs, reducing wingtip shed vorticity, and therefore induced drag, may also reduce global warming because of the lower fuel consumption. The world's commercial jet aircraft generate more than 600 million tons of carbon dioxide per year[8].

The techniques for its tip vortices reduction include winglets, wingtip sails, Raked wing tips and Ogee tips. Much of the development work for the winglet was initiated by Whitcomb at NASA [9, 10].

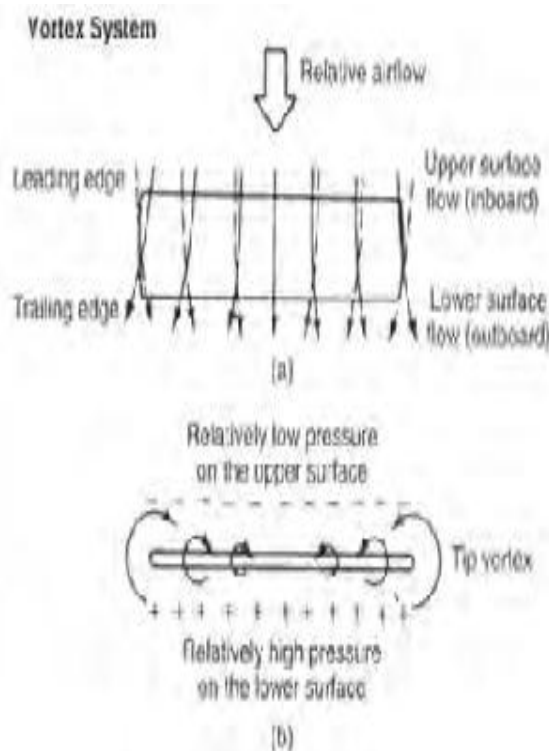


**Fig. 1.** Pressure equalization on the wing tip and vortices.

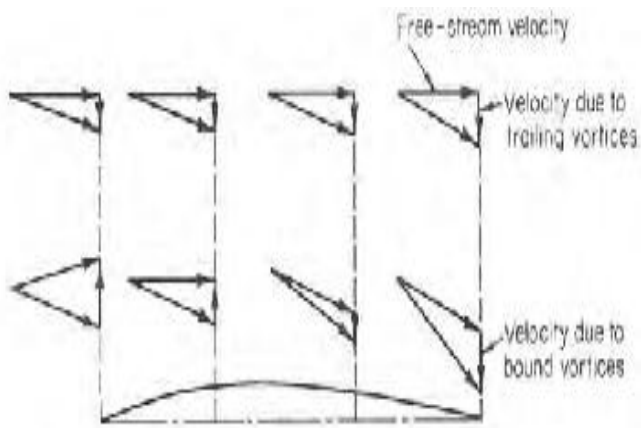


Fig. 2. Downwash due to bound and trailing vortices.

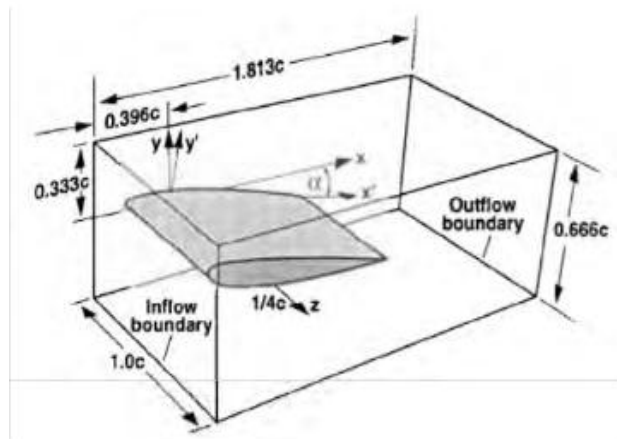


Fig. 3. Domain.

This paper presents the validation of CFD code against NASA experiments data and then to find the variation of the circulation at different areas to the right of the wingtip vortex core and tangential velocity at one chord downstream of the trailing edge is obtained. Also shows the reduction of wing tip vortex by applying suction on the wing tip.

## II. PROCEDURE

### A. Overview

This paper presents a comparison between wingtip vortex flow field done by CFD simulations and experimental measurements done at NASA by Chow et al., [11] as a validation of the present numerical CFD simulations and several different configurations have been taken to explore their potential to reduce the wing tip vortex qualitatively.

The present simulations were run in ANSYS 13.0, which models fluid flow and heat transfer problems in complex geometries. This commercial CFD software solves the general transport equations using the finite volume method. Steady-state, transient, incompressible, compressible, inviscid, viscous, laminar, and turbulent flows can be solved with Fluent.

### B. Complete Geometry Case

The computational domain includes a half-wing inside a wind tunnel (Fig. 3) such as the one used by Chow et al., [11] The model is a rectangular wing with an aspect ratio of 1.5, 4 ft chord and 3 ft. half span. The airfoil section is a NACA 0012 at  $10^\circ$  angle of attack. The dimensions of the wind tunnel test section are 32x48 in. Free stream velocity is 170 ft/s yielding a chord Reynolds number of  $4.6 \times 10^6$ .

Here the wing tip used was a rounded wing tip to get the vortex centered around the wing tip. Rounded wing tip provides better aerodynamic performance compared to squared wing tips. To get attached flow over the wing, strips were used as done by Chow et al., [11] Because at higher angle of attack, the flow is separated at the top of the wing. This separation causes additional drag and also tends to stall. To prevent these, strips was placed across the span of the wing at a distance of 0.1666 ft. ( 2 in.) from the leading edge and it has a width of 0.010416 ft. (0.125 in.). The strip extended around the tip and along the bottom surface of the wing (Fig. 4)

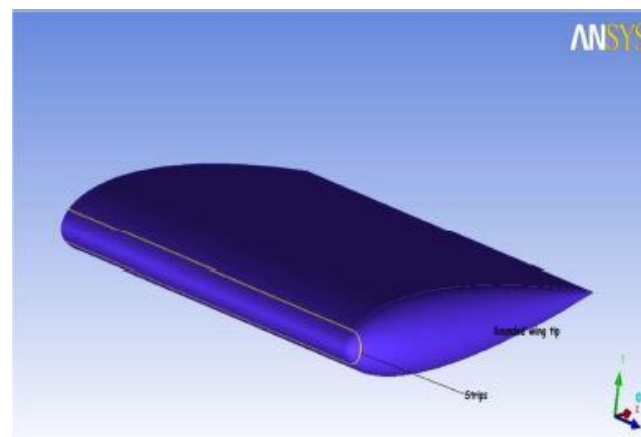


Fig. 4. Wing with strips.

### C. Mesh generation

The geometry was imported to ANSYS ICEM CFD to generate meshes. ANSYS ICEM CFD provides advanced geometry acquisition, mesh generation, mesh optimization, and post-processing tools to meet the requirement for integrated mesh generation and post processing tools for today's sophisticated analyses. Maintaining a close relationship with the geometry during mesh generation and post-processing, ANSYS ICEM CFD is used especially in engineering applications such as computational fluid dynamics and structural analysis.

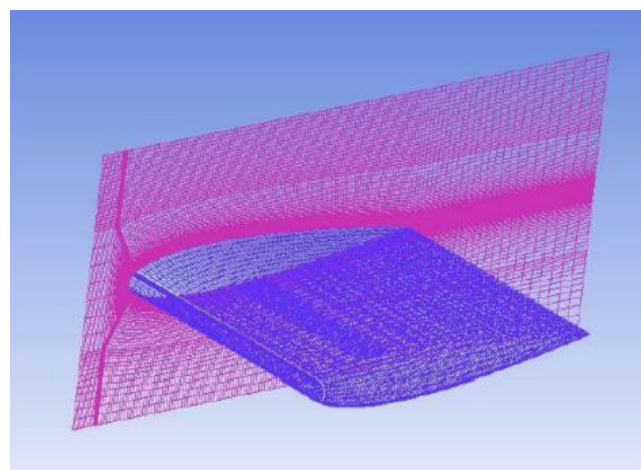


Fig. 5. Wing and wing-root wall surface with structured grids.

#### D. Solver configuration

After generating mesh it was feed to a solver to calculate the flow properties. Here the solver used was a FLUENT. ANSYS FLUENT is a state-of-the-art computer program for modeling fluid flow, heat transfer, and chemical reactions in complex geometries. ANSYS FLUENT uses a client/server architecture, which allows it to run as separate simultaneous processes on client desktop workstations and powerful computer servers. This architecture allows for efficient execution, interactive control, and complete flexibility between different types of machines or operating systems. ANSYS FLUENT provides complete mesh flexibility, including the ability to solve the flow problems using unstructured meshes that can be generated about complex geometries with relative ease. Supported mesh types include 2D triangular/quadrilateral, 3D tetrahedral /hexahedral / pyramid / wedge/ polyhedral, and mixed (hybrid) meshes. ANSYS FLUENT also allows to refine or coarsen the mesh based on the flow solution.

#### E. Boundary Conditions

The inlet boundary condition was defined as a uniform inlet velocity =170 ft/s. The outlet boundary condition was based on a pressure outlet condition. The wind tunnel walls were defined as slip walls with a uniform velocity of  $V_\infty$ , except on the wall of symmetry, where the normal velocity component were set equal to zero. The wing surface was defined as a stationary surface.

#### F. Circulation across the Wingtip Vortex

The circulation, denoted by  $\Gamma$  is defined as [12].

$$\Gamma = - \oint \mathbf{V} \cdot d\mathbf{s} = - \iint (\nabla \times \mathbf{V}) \cdot d\mathbf{s}$$

Minus sign appears in above equation to account for positive-counter clockwise sense of the integral and positive-counter clockwise sense of the circulation

For a plane it becomes [13]:

$$\Gamma = \oint (u dx + v dy) = \iint \left( \frac{\partial v}{\partial x} - \frac{\partial u}{\partial y} \right) dx dy$$

Where equation of vorticity ( $\zeta$ ) is

$$\left( \frac{\partial v}{\partial x} - \frac{\partial u}{\partial y} \right) = \zeta$$

Where u is the velocity component in the x-direction and v is the velocity component in the y-direction. The simulation is obtained at an angle of attack of 10 for different x/c locations and result is presented in Table -1 (Fig. – 8).

### III. RESULTS AND DISCUSSION

#### A. Validation of the CFD code

Pressure coefficient contours at vortex for different locations(x/c) are computed at 10° angle of attack and free stream velocity of 170 ft/s and compared with the experimental measurements done at NASA by Chow et al.,[11] Fig. 6 displays at various cross flow planes (x/c = 0.7, 0.8, 0.9, 1.0, 1.2 and 1.4).

Fig. 6 and 7 shows a comparison between pressure coefficient ( $C_p$ ) and axial velocity measurements done by Chow et al. and simulations done in Fluent. The simulations show good agreement with the experimental data.

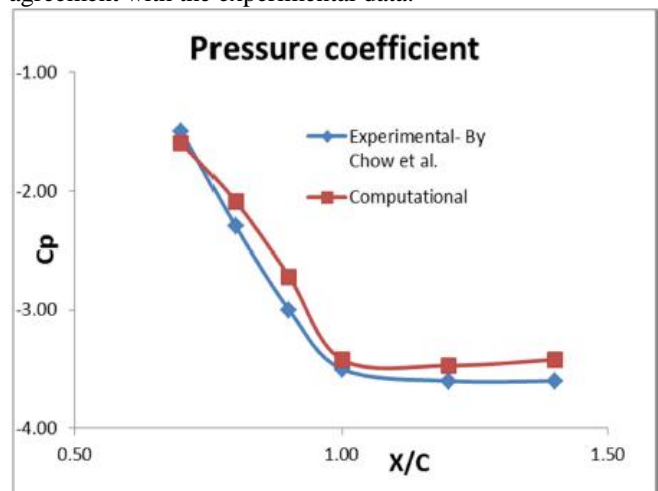


Fig.6. Pressure coefficient in the wing tip vortex core in the downstream direction.

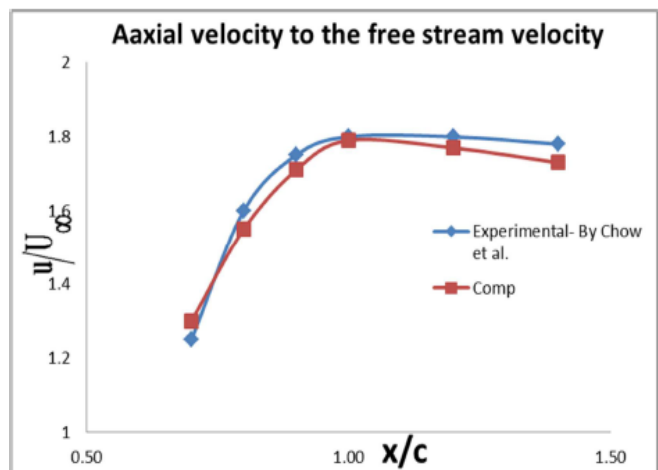


Fig.7. Axial velocity in the wing tip vortex core in the downstream direction.

Several rectangles were taken with different size to the right of the wingtip vortex core to compute the circulation and know how it changes (Fig. 8). Rectangles were drawn taking different distances from the right of the wingtip vortex core at one chord downstream of the trailing edge. The circulation, or vortex strength, was calculated either by a line integral over the velocity and by the area integral over vorticity. No

noticeable difference was found between these two calculation methods. In this paper line integral method is used to find out the circulation. Table 1 shows the circulation values at different areas to the right of the vortex core at one chord downstream of the trailing edge of a NACA 0012 wing.

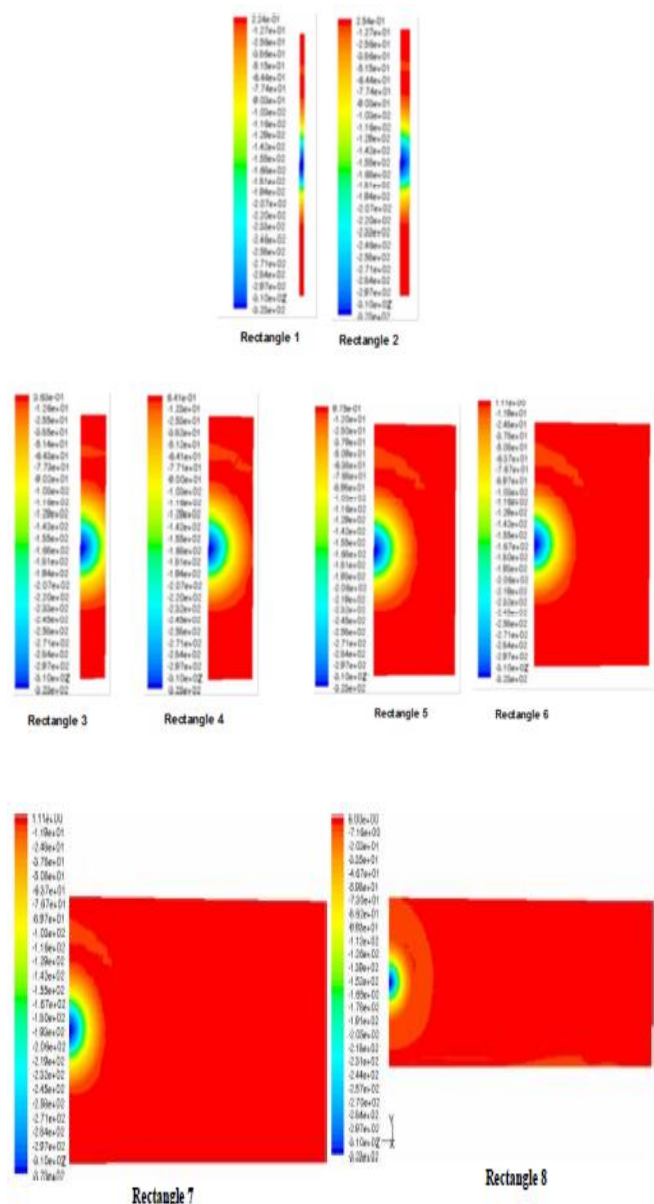


Fig. 8. Different rectangles size from the right of the vortex core to compute the circulation.

Contour	Distance (m) from the vortex core	Circulation (m <sup>2</sup> /s)
1	0.007	0.1551481
2	0.014	0.3112252
3	0.022	0.4394314
4	0.037	0.5982956
5	0.067	0.6837664
6	0.128	0.7088502
7	0.189	0.7357921
8	0.494	0.7896758

Table 1. Variation of circulation at different areas, right of the

vortex core.

The variation of the circulation at different rectangles from right of the vortex core is drawn in Fig. 9. It shows that the circulation approaches to an asymptotic value at 0.08 m from vortex core.

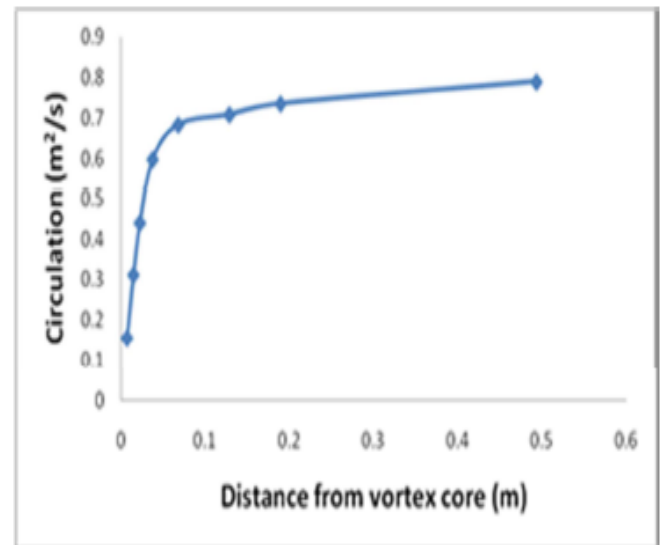


Fig. 9. Circulation at different rectangles from the right of a wingtip vortex core.

Several square contours were drawn around the wingtip vortex core in order to compute the total circulation strength. Figure 10 shows the variation of total circulation strength around the vortex core are increased. Notice that the magnitude of the total circulation strength are approximately twice of the circulation when measured from the right of vortex core.

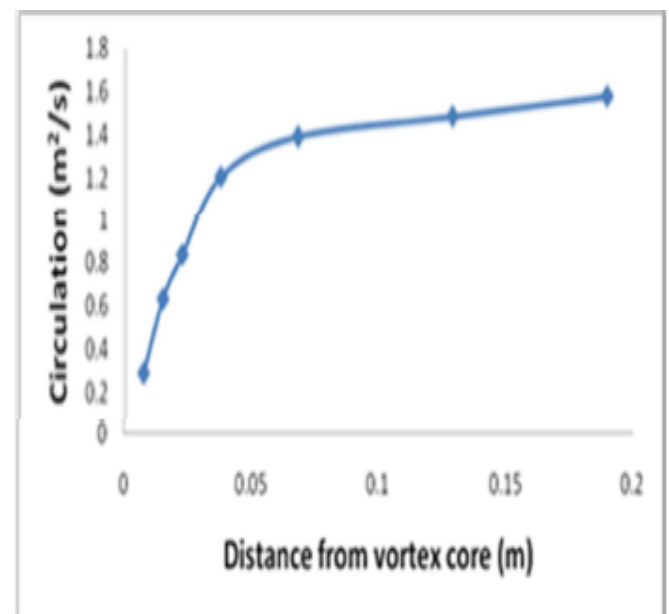


Fig. 10. Total circulation variation with distance from the vortex core.

The variation of non-dimensional (tangential velocity to free stream velocity,  $U_{\theta}/U_{\infty}$ ) along the wingtip

vortex core of a NACA 0012 wing at one chord downstream of the trailing edge is shown in Fig. 11 The variation of non-dimensional (tangential velocity to free stream velocity,

$U_{\theta}/U_{\infty}$ ) along the wingtip

vortex core of a NACA 0012 wing at one chord downstream of the trailing edge is shown in Fig. 11.

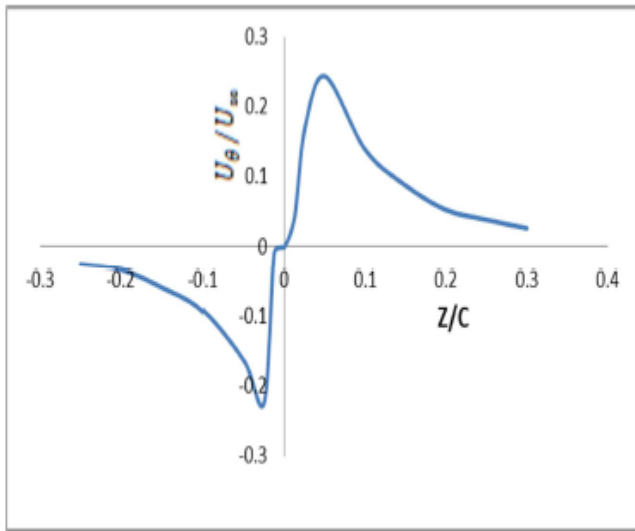


**Fig. 11.** Variation tangential velocity to free stream velocity ( $U_{\theta}/U_{\infty}$ ) velocity along the wingtip vortex core.

#### IV. CONCLUSION

Numerical simulations done in the current study to reproduce the experimental measurements done by Chow et al., [11] at NASA has shown very good agreement in predicting the formation of wing tip vortices, and also good agreement for pressure coefficient values are obtained.

The strength of the circulation increases with the area from right of the vortex core and attains a maximum value and remains close to constant after a particular distance (0.08 m). The circulation approaches an asymptotic value after certain distance from the vortex core. The tangential velocity of vortex increases rapidly with the distance from the vortex core and approaches a maximum at 7 percent of chord from the vortex core. The magnitude of tangential velocity starts reducing slowly after 7 percent of chord from the vortex core.

It is concluded based on the present study that tip-vortices, which are one of the most prominent aspects of lifting surface flows yet have been perceived difficult to tackle numerically, are tractable indeed with modern.

CFD code and can be predicted with a good accuracy. The wing tip vortex, which is the cause of induce drag can be nullified using correct combination of suction and blowing at appropriate location.

#### REFERENCES:

- [1] Bertin, J. J. and Smith, M. L., Aerodynamics for Engineers 3rd Edition, Prentice Hall, Upper Saddle River, NJ 1998.
- [2] Stinton, D., The Design of the Aeroplane 2nd Edition, Blackwell publishing, London, Great Britain 2003.
- [3] Hoerner, S.F., Fluid Dynamic Drag Theoretical, Experimental and Statistical Information, Published by the author, Brick Town, N.J. 1965.
- [4] Zimmer, H.: Aerodynamic Optimization of Wings at Subsonic Speeds and the Influence of Wingtip Design. NASA TM-88534, 1983.
- [5] Thomas, A. S., "Aircraft Drag Reduction Technology – A Summary," Advisory Group for Aerospace Research and Development (AGARD), Report 723, Belgium, 1985.
- [6] Airguide, "Jet Aircraft World Fleet Summary," Air Guide Online. 2006. <[http://www.airguideonline.com/aircr\\_wfleet.htm](http://www.airguideonline.com/aircr_wfleet.htm)> (4 May 2006).
- [7] Kroo, I. "Nonplanar Wing Concepts for Increased Air craft Efficiency," VKI Lecture Series on Innovative Configurations and Advanced Concepts for Future Civil Aircraft, Stanford, 2005.
- [8] Barnett, A., "Pace hots up in a World forever n the move," Guardian Unlimited. 2006. <<http://observer.guardian.co.uk/carbontrust/story/0,16099,1511925,00.html>> (4 May 2006).
- [9] Whitcomb, R., "A Design Approach and Selected Wind- Tunnel Results at High Subsonic Speeds for Wing Tip mounted Winglets," NASA TN-D-8260, 1976.
- [10] Whitcomb, R.T., "Methods for reducing subsonic drag due to lift," Special course on concepts for drag reduction, AGARD, France 1977, pp. 2-1 to 2-11
- [11] Chow, J., Zilliac, G., and Bradshaw, P., "Mean Turbulence Measurements in the Nearfield of a Wingtip Vortex," AIAA JOURNAL Vol. 35, No. 10, October 1997
- [12] John D Anderson Jr, "Fundamental of Aerodynamics", Fifth Edition. McGraw Hill.
- [13] E L Houghton and N B Carruthers, "Aerodynamics for Engineering Students" Third Edition.